Acta Cryst E CRYSTALLOGRAPHIC COMMUNICATIONS

ISSN 2056-9890

Cooperative *sp* C—H···N and sp^2 C—H···N hydrogen bonding in the 1:1 cocrystal 1,2-bis(pyrimidin-5-yl)ethyne–2,6-diethynylpyridine

Eric Bosch*

Department of Chemistry and Biochemistry, Missouri State University, 901 South National Avenue, Springfield MO 65897, USA. *Correspondence e-mail: ericbosch@missouristate.edu

Received 1 October 2026
Accepted 26 October 2026

Edited by J. Reibenspies, Texas A & M University, USA

Keywords: crystal structure; sp^2-C—H···N hydrogen bond; *sp*-C—H···N hydrogen bond; sp^2-C—H···C(alkyne) interaction; 2,6-diethynyl pyridine; 1,2-*bis*(pyrimidin-5-yl)ethyne.

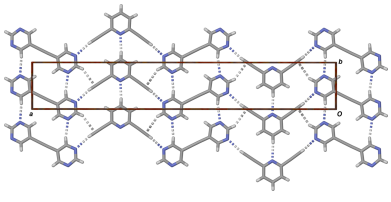
CCDC reference: 2598229

Supporting information: this article has supporting information at journals.iucr.org/e

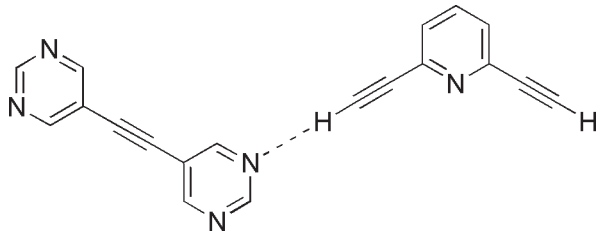
The title cocrystal $C_{10}H_6N_4{\cdot}C_9H_5N$, crystalizes in the monoclinic space group $Pna2_1$ with two molecules of each component in the asymmetric unit. The extended structure features four unique *sp*-C—H···N interactions between components that form zigzag hydrogen-bonded chains along the *a*-axis direction. Complementary pyridine and pyrimidine C—H···N bonds along the *b*-axis direction result in the formation of planar two-dimensional sheets. A Hirshfeld surface analysis and calculation of intermolecular interaction energies within the crystal structure are reported.

1. Chemical context

Early reports that suggested the existence of C—H···O hydrogen bonds within crystal structures (Sutor, 1962) were confirmed and comprehensively reviewed several decades ago (Desiraju, 1996; Steiner, 2003). Currently, C—H hydrogen bonding is widely accepted in both chemical and biochemical fields (Derewenda, 2023). We initially studied terminal alkynes as C—H hydrogen-bond donors since hydrogen atoms bonded to *sp*-C atoms are more polarized, exhibiting a pK_a of approximately 25. We first focussed on *sp*-C—H···N(pyridine) interactions and noted that the vast majority of the published examples were reported in crystal structures of single molecules that included both a terminal alkyne and an amine donor. We chose to investigate the potential of these C—H···N hydrogen bonds to induce the formation of cocrystals between 1,4-diethynyl benzenes and aromatic amines like 1,2-bis(4-pyridyl)ethyne (Bosch, 2010, 2026). We, and others, investigated the role of phenyl C—H···N hydrogen bonds in cocrystals between fluorinated benzenes and pyridines (Bosch *et al.*, 2015; Präsang *et al.*, 2013). Here we present the cocrystallization of 1,2-bis(pyrimidin-5-yl)ethyne (**BPE**) with 2,6-diethynylpyridine (**DEP**). We expected that we would form cocrystals with π-stacked planar sheets comprising multiple cooperative *sp* and sp^2-C—H···N hydrogen bonds. This was based on our knowledge of both *sp*-C—H···N hydrogen bonding and sp^2-C—H···N hydrogen bonding of pyridines and pyrimidines within the crystal structure of 1,2-bis(pyrimidin-5-yl)ethyne and its cocrystals with 2,6-*bis*(iodoethynyl)pyridine (Lang *et al.*, 2024).



OPEN ACCESS
Published under a CC BY 4.0 licence



2. Structural commentary

The asymmetric unit of the cocrystal **BPE·DEP** contains two unique molecules of each component as shown in Fig. 1. The two hydrogen-bonded pairs of molecules are in adjacent planes separated by 3.3 Å. The two **BPE** molecules are almost planar with dihedral angles between the pyrimidine rings in each of about 7°. The associated **DEP** molecules are slightly out of the plane defined by each C—H···N hydrogen-bonded **BPE**.

3. Supramolecular features

The two-dimensional planar sheet of **BPE·DPE** as shown in Fig. 2 features alternating rows of **BPE** molecules and **DPE** molecules along the direction of the *b* axis. The **BPE** molecules within each row are held together by self-complementary pyrimidine–pyrimidine sp^2-C—H···N hydrogen bonds with four hydrogen bonds between each pair of **BPE** molecules. The **DEP** molecules within each row feature a single pyridine-pyridine sp^2-C—H···N hydrogen bond. The *sp*-C—H···N (pyrimidine) hydrogen bonds effectively zipper the alternating rows together. The ten unique C—H···N hydrogen bonds are collated in Table 1. The first four entries in Table 1 correspond to the *sp*-C—H···N separations that range from 2.46 to 2.51 Å, 84 to 91% of the sum of the van der Waals radii (Bondi, 1964). There is a weak supporting C—H···π interaction between the pyrimidine C—H between the two N atoms and each alkyne (Fig. 2) with H···C separations ranging from 2.78 to 2.88 Å at 96–99% of the sum of the van der Waals radii. The *sp*-C—H···N hydrogen bonds, entries 5 to 8 in Table 1, have H···N separations between 2.32 and 2.47 Å and the pyridine–pyridine sp^2C—H···N hydrogen bonds have H···N separations of 2.38 and 2.39 Å. These planar sheets are, indeed, like those we observed in the cocrystal between 2,6-*bis*(iodoethynyl)pyridine and **BPE** (Lang *et al.*, 2024).

These planar sheets are π-stacked along the *c*-axis direction as illustrated in Fig. 3, which shows the slightly corrugated nature of the sheets.

The Hirshfeld surface for one of the unique **BPE** molecules within the cocrystal was calculated with *CrystalExplorer 17* (Spackman *et al.*, 2021). Fig. 4 shows the five molecules in close contact to the central **BPE** and highlights the close contacts corresponding to the C—H···N hydrogen bonds in red.

The close contacts derived from the Hirshfeld plot were analysed in terms of specific atom-to-atom contacts and the fingerprint plots in Fig. 5 calculated. The plot corresponding to all atom-to-atom contacts is shown in Fig. 5(*a*). H···H contacts, shown in Fig. 5(*c*), correspond to 30.5% of the surface area contacts. N···H/H···N and C···H/H···C contacts, Fig. 5(*b*) and 5(*d*), correspond 27.7 and 22.1% of the surface area, respectively. The C···C and C···N interactions that are predominantly π-stacking interactions, correspond to 10.3 and 7.8% of the surface area respectively. These latter interactions have atom-to-atom distances concentrated around 3.6 Å and appear as the central teal area in Fig. 5 (*a*).

The intermolecular energy of interaction of neighbouring molecules within the crystal structure were calculated for each molecule in the asymmetric unit. Each of the major interactions is shown in Fig. 6. Thus the molecule labelled **Y** has two cooperative sp^2-C—H···N hydrogen bonds to the central **BPE**, labelled '*b*' in Fig. 6. The average energy of interaction

Table 1
Hydrogen-bond geometry (Å, °).

D—H···*A*	*D*—H	H···*A*	*D*···*A*	*D*—H···*A*
C10—H10···N3^{i}	0.95	2.50	3.423 (6)	165
C17—H17···N5^{ii}	0.95	2.49	3.420 (6)	166
C20—H20···N7^{i}	0.95	2.46	3.405 (6)	171
C27—H27···N9^{ii}	0.95	2.51	3.436 (6)	164
C1—H1···N4^{iii}	0.95	2.44	3.380 (6)	170
C9—H9···N2	0.95	2.33	3.260 (5)	165
C30—H30···N8	0.95	2.47	3.380 (6)	160
C38—H38···N6^{iv}	0.95	2.32	3.268 (6)	175
C5—H5···N1^{i}	0.95	2.38	3.331 (6)	176
C34—H34···N10^{ii}	0.95	2.39	3.336 (6)	175

Symmetry codes: (i) $x, y+1, z$; (ii) $x, y-1, z$; (iii) $x+\frac{1}{2}, -y+\frac{1}{2}, z$; (iv) $x-\frac{1}{2}, -y+\frac{3}{2}, z$.

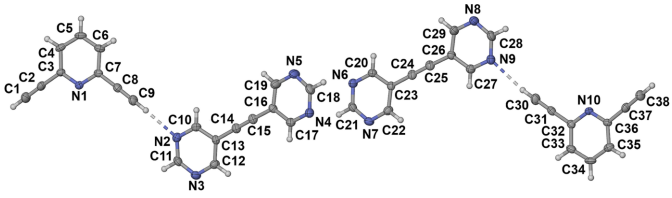


Figure 1
Labeled asymmetric unit of the cocrystal, **BPE·DEP**, with displacement ellipsoids drawn at the 50% level. C—H···N hydrogen bonds shown as dashed lines.

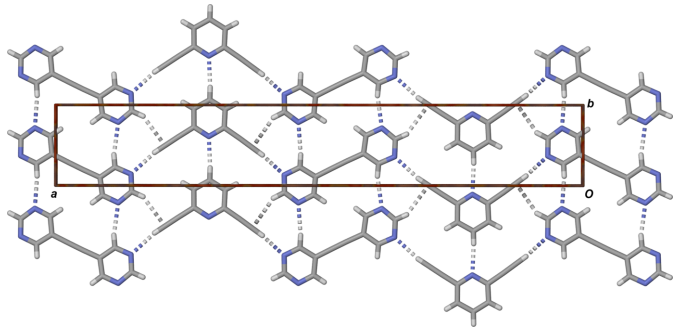


Figure 2
View, along the *c*-axis, of one of the two unique planar sheets of alternating C—H···N and C—H···C hydrogen bonded molecules within the cocrystal **BPE·DEP**.

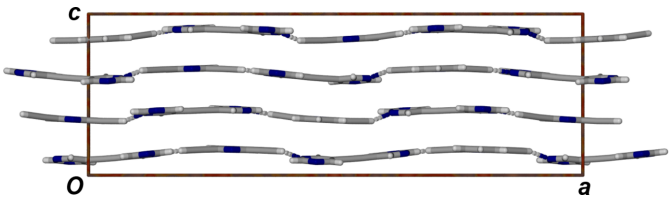


Figure 3
View of the unit cell packing of the cocrystal **BPE·DEP** along the *b* axis.

between the two **BPE** molecules is −21.4 kJmol^{-1}. The **DEP** molecule labelled **T** in Fig. 6 has an *sp*-C—H···N interaction, labelled 'c', with the central **DPE** molecule. The average energy of this interaction for the four unique alkynes is −12.7 kJmol^{-1}. The π-stacked **DEP** molecule labelled **G** has large surface area of interaction with one alkyne lying along the **BPE** with the close C···C contact labelled 'd' with an average intermolecular energy of interaction of −28.5 kJmol^{-1}. The **DEP** molecule labelled **R** has an sp^2-C—H···alkyne interaction labelled 'e' with an average energy of interaction between these molecules of 8.0 kJmol^{-1}. The C···C separation for 'e' is 3.37 Å. Also shown in Fig. 6 is the sp^2-C—H···N hydrogen bond 'a' between pyridines labelled **P** and **G** with an average interaction energy of 12.7 kJmol^{-1}.

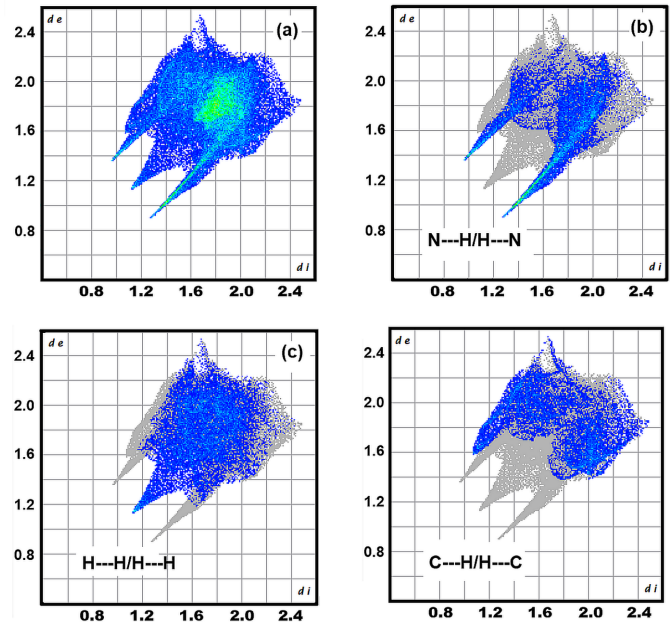


Figure 5
Two-dimensional fingerprint plots showing the contributions of the major interactions to the total Hirshfeld surface area of a **BPE** in the cocrystal. (*a*) All atom-atom interactions, (*b*) N···H/H···N interactions, (*c*) H···H/H···H interactions and (*d*) C···H/H···C interactions.

4. Database survey

A search of the Cambridge Crystallographic Database (Version 2026.1.0; Groom *et al.*, 2016) using Conquest Build 483767 (Bruno *et al.*, 2002) for structures containing the **DPE** yielded 11 structures. Two of these are the structure of **DPE** alone, refcode AZEDAN (Meitinger *et al.*, 2021) and AZEDAN01 (Lang *et al.*, 2024). The coordination complexes formed between **DPE** and copper(I) iodide and bromide, refcodes LUMJEI and LUMJIM, were reported (Georgiev *et al.*, 2001) as were hydrogen-bonded complexes formed between **DPE** and C-methyl resorcinarene, refcodes PAQYIQ, PAQYOW and PAQYUC (Georgiev *et al.*, 2004). Recently we formed a halogen-bonded cocrystal of **DPE** with 1,3-diiodotetrafluorobenzene, refcode PUZGUP (Nwachukwu *et al.*, 2020) and three halogen-bonded cocrystals of **DPE** with the isomeric bis(iodoethynyl)pyridines, refcodes UGUKOA, UGULAN and UGULIV (Lang *et al.*, 2024). It is noteworthy that self-complementary pyrimidine–pyrimidine C—H···N hydrogen bonding, the strongest intermolecular interaction in the cocrystal **DPE·DEP**, is observed in the structures of **DPE** alone and in the halogen-bonded cocrystals of **DPE**. There are three structures of **DEP** in the database. **DEP** alone is refcode IDUWEJ (Ohkita *et al.*, 2001), the cocrystal of **DEP** with 5-ethynylpyrimidine is refcode RUXNAA (Bosch, 2010). In these structures there are pyridine–pyridine C—H···N hydrogen bonds as observed in cocrystal and the cocrystal **DPE·DEP**. Also the cocrystal of

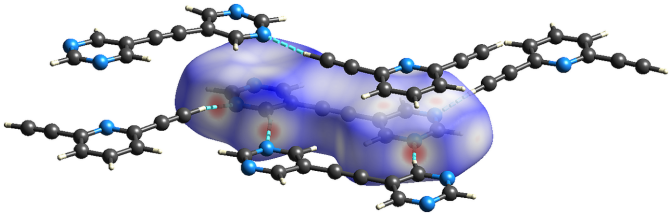


Figure 4
Hirshfeld surface of one of the unique **BPE** molecules and the 5 molecules making close contact. CH···N hydrogen bonds shown as dashed lines.

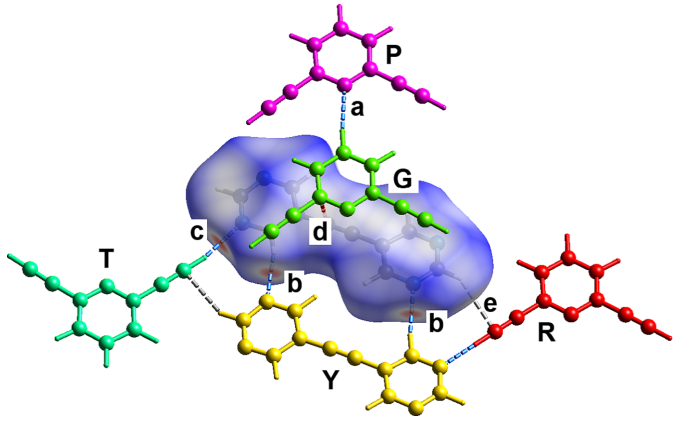


Figure 6
Color-coded molecules, within 3.8 Å of a central **DPE** molecule in cocrystal **(DPE·DEP)**, that have significant attractive intermolecular energies of interaction with interactions labelled and shown as dashed lines. Labels are; **a** pyridine-pyridine C—H···N, **b** pyrimidine-pyrimidine C—H···N, **c** alkyne C—H···N, **d** π-stacking C···C, **e** pyrimidine C—H···alkyne. Molecule labels (colours) are: **Y** (yellow), **T** (turquoise), **G** (green), **P** (pink) and **R** (red).

DEP with *N*-iodosuccinimide is refcode DEGTAO (Bosch & Bowling, 2022).

5. Synthesis and crystallization

The compounds used in this study were available from previous studies (Lang *et al.*, 2024). Equimolar amounts, 0.1 mmol, of each component were weighed and placed in a small screw-cap vial and 2 mL of dichloromethane were added to effect complete solution of both compounds. The lid was loosely attached to permit slow evaporation of the solvent as a homogeneous mass of colourless plates formed.

6. Refinement

Crystal data, data collection and structure refinement details are summarized in Table 2. H atoms were positioned geometrically (C—H = 0.95 Å) and refined as riding with U_{iso}(H) = 1.2U_{eq}(C).

Acknowledgements

The Missouri State University Provost Incentive Fund funded the purchase of the X-ray diffractometer.

Table 2
Experimental details.

Crystal data	
Chemical formula	$C_{10}H_6N_4{\cdot}C_9H_5N$
M_r	309.33
Crystal system, space group	Orthorhombic, $Pna2_1$
Temperature (K)	173
a, b, c (Å)	40.053 (4), 6.1144 (6), 12.9933 (13)
V (Å^3)	3182.1 (5)
Z	8
Radiation type	Mo $K\alpha$
μ (mm^{-1})	0.08
Crystal size (mm)	0.60 × 0.20 × 0.05
Data collection	
Diffractometer	Bruker APEXI CCD
Absorption correction	Multi-scan (*SADABS*; Krause *et al.*, 2015))
T_{min}, T_{max}	0.672, 0.746
No. of measured, independent and observed [$I > 2\sigma(I)$] reflections	35545, 6501, 4000
R_{int}	0.075
(sin $\theta/\lambda)_{max}$ (Å^{-1})	0.625
Refinement	
$R[F^2 > 2\sigma(F^2)]$, $wR(F^2)$, S	0.049, 0.119, 1.01
No. of reflections	6501
No. of parameters	434
No. of restraints	1
H-atom treatment	H-atom parameters constrained
$\Delta\rho_{max}$, $\Delta\rho_{min}$ (e Å^{-3})	0.20, −0.15

Computer programs: *SMART* and *SAINT* (Bruker, 2014), *SHELXT2018/2* (Sheldrick, 2015*a*), *SHELXL2019/3* (Sheldrick, 2015*b*) and *X-SEED* (Barbour, 2020).

References

Barbour, L. J. (2020). *J. Appl. Cryst.* **53**, 1141–1146.
Bondi, A. (1964). *J. Phys. Chem.* **68**, 441–451.
Bosch, E. (2010). *Cryst. Growth Des.* **10**, 3808–3813.
Bosch, E. (2026). *J. Chem. Crystallogr.* **56**, 35.
Bosch, E. & Bowling, N. P. (2022). *Acta Cryst.* C**78**, 424–429.
Bosch, E., Bowling, N. P. & Darko, J. (2015). *Cryst. Growth Des.* **15**, 1634–1641.
Bruker (2014). *SMART* and *SAINT*. Bruker AXS Inc., Madison, Wisconsin, USA.
Bruno, I. J., Cole, J. C., Edgington, P. R., Kessler, M., Macrae, C. F., McCabe, P., Pearson, J. & Taylor, R. (2002). *Acta Cryst.* B**58**, 389–397.
Derewenda, Z. S. (2023). *Int. J. Mol. Sci.* **24**, 13165.
Desiraju, G. R. (1996). *Acc. Chem. Res.* **29**, 441–449.
Georgiev, I., Barnes, C. L. & Bosch, E. (2001). *J. Supramol. Chem.* **1**, 153–155.
Georgiev, I., Bosch, E., Barnes, C. L. & Draganjac, M. (2004). *Cryst. Growth Des.* **4**, 235–239.
Groom, C. R., Bruno, I. J., Lightfoot, M. P. & Ward, S. C. (2016). *Acta Cryst.* B**72**, 171–179.
Krause, L., Herbst-Irmer, R., Sheldrick, G. M. & Stalke, D. (2015). *J. Appl. Cryst.* **48**, 3–10.
Lang, L. B., Bowling, N. P. & Bosch, E. (2024). *Cryst. Growth Des.* **24**, 9727–9734.
Meitinger, N., Mengele, A. K., Nauroozi, D. & Rau, S. (2021). *Org. Mater.* **3**, 295–302.
Nwachukwu, C. I., Patton, L. J., Bowling, N. P. & Bosch, E. (2020). *Acta Cryst.* C**76**, 458–467.
Ohkita, M., Suzuki, T., Nakatani, K. & Tsuji, T. (2001). *Chem. Lett.* **30**, 988–989.
Präsang, C., McAllister, L. J., Whitwood, A. C. & Bruce, D. W. (2013). *CrystEngComm* **15**, 8947–8958.
Sheldrick, G. M. (2015*a*). *Acta Cryst.* C**71**, 3–8.
Sheldrick, G. M. (2015*b*). *Acta Cryst.* A**71**, 3–8.
Spackman, P. R., Turner, M. J., McKinnon, J. J., Wolff, S. K., Grimwood, D. J., Jayatilaka, D. & Spackman, M. A. (2021). *J. Appl. Cryst.* **54**, 1006–1011.
Steiner, T. (2003). *Crystallogr. Rev.* **9**, 177–228.
Sutor, D. J. (1962). *Nature* **195**, 68–69.

supporting information

Acta Cryst. (2026). E**82**, 1376-1379 [https://doi.org/10.1107/S2056989026011102]

Cooperative *sp* C—H···N and sp^2 C—H···N hydrogen bonding in the 1:1 cocrystal 1,2-bis(pyrimidin-5-yl)ethyne–2,6-diethynylpyridine

Eric Bosch

Computing details

(I)

Crystal data

$C_{10}H_6N_4 \cdot C_9H_5N$
$M_r = 309.33$
Orthorhombic, $Pna2_1$
$a = 40.053$ (4) Å
$b = 6.1144$ (6) Å
$c = 12.9933$ (13) Å
$V = 3182.1$ (5) Å^3
$Z = 8$
$F(000) = 1280$
$D_x = 1.291$ Mg m^{-3}
Mo $K\alpha$ radiation, $\lambda = 0.71073$ Å
Cell parameters from 3041 reflections
$\theta = 2.6$–$26.0°$
$\mu = 0.08$ mm^{-1}
$T = 173$ K
Plate, colourless
0.60 × 0.20 × 0.05 mm

Data collection

Bruker APEXI CCD diffractometer
Radiation source: fine-focus sealed tube
Graphite monochromator
Detector resolution: 8.3660 pixels mm^{-1}
phi and ω scans
Absorption correction: multi-scan (SADABS; Krause *et al.*, 2015))
$T_{min} = 0.672$, $T_{max} = 0.746$
35545 measured reflections
6501 independent reflections
4000 reflections with $I > 2\sigma(I)$
$R_{int} = 0.075$
$\theta_{max} = 26.4°$, $\theta_{min} = 2.6°$
$h = -50 \rightarrow 50$
$k = -7 \rightarrow 7$
$l = -16 \rightarrow 16$

Refinement

Refinement on F^2
Least-squares matrix: full
$R[F^2 > 2\sigma(F^2)] = 0.049$
$wR(F^2) = 0.119$
$S = 1.01$
6501 reflections
434 parameters
1 restraint
Primary atom site location: dual
Hydrogen site location: inferred from neighbouring sites
H-atom parameters constrained
$w = 1/[\sigma^2(F_o^2) + (0.0462P)^2 + 0.3002P]$ where $P = (F_o^2 + 2F_c^2)/3$
$(\Delta/\sigma)_{max} < 0.001$
$\Delta\rho_{max} = 0.20$ e Å^{-3}
$\Delta\rho_{min} = -0.15$ e Å^{-3}
Extinction correction: SHELXL-2019/3 (Sheldrick 2015b)
Extinction coefficient: 0.0008 (2)

Special details

Geometry. All esds (except the esd in the dihedral angle between two l.s. planes) are estimated using the full covariance matrix. The cell esds are taken into account individually in the estimation of esds in distances, angles and torsion angles; correlations between esds in cell parameters are only used when they are defined by crystal symmetry. An approximate (isotropic) treatment of cell esds is used for estimating esds involving l.s. planes.

Fractional atomic coordinates and isotropic or equivalent isotropic displacement parameters (Å²)

	x	*y*	*z*	U_{iso}*/U_{eq}
N1	0.70954 (7)	0.6089 (6)	0.3405 (3)	0.0286 (9)
C1	0.79271 (11)	0.4959 (7)	0.3440 (4)	0.0453 (12)
H1	0.812495	0.410429	0.346813	0.054*
N2	0.56656 (8)	0.1314 (6)	0.3982 (3)	0.0360 (9)
C2	0.76830 (10)	0.6014 (7)	0.3405 (4)	0.0338 (10)
N3	0.53964 (9)	−0.2145 (6)	0.4163 (3)	0.0377 (10)
C3	0.73771 (9)	0.7267 (6)	0.3384 (3)	0.0273 (9)
N4	0.35714 (8)	0.3586 (6)	0.3636 (3)	0.0387 (9)
C4	0.73803 (11)	0.9546 (7)	0.3363 (3)	0.0352 (11)
H4	0.758488	1.032857	0.333021	0.042*
N5	0.38130 (9)	0.7146 (6)	0.3674 (3)	0.0469 (11)
C5	0.70769 (11)	1.0643 (8)	0.3393 (4)	0.0404 (11)
H5	0.707099	1.219661	0.339138	0.048*
N10	−0.03096 (8)	0.3847 (6)	0.6537 (3)	0.0279 (9)
C6	0.67862 (11)	0.9464 (7)	0.3425 (4)	0.0369 (11)
H6	0.657628	1.018548	0.344935	0.044*
N6	0.32429 (8)	0.6352 (6)	0.5975 (3)	0.0346 (9)
C7	0.68039 (9)	0.7191 (7)	0.3421 (3)	0.0285 (9)
N7	0.29795 (9)	0.2857 (6)	0.5884 (3)	0.0354 (9)
C8	0.65084 (10)	0.5856 (7)	0.3449 (4)	0.0324 (10)
N8	0.11432 (8)	0.8539 (6)	0.6121 (3)	0.0368 (9)
C9	0.62710 (10)	0.4715 (7)	0.3483 (4)	0.0400 (11)
H9	0.607994	0.379638	0.350950	0.048*
N9	0.13825 (8)	1.2079 (6)	0.5975 (4)	0.0467 (10)
C10	0.53651 (10)	0.2276 (8)	0.3964 (4)	0.0326 (11)
H10	0.535352	0.382122	0.389686	0.039*
C11	0.56605 (11)	−0.0857 (8)	0.4072 (4)	0.0376 (12)
H11	0.587164	−0.156537	0.407103	0.045*
C12	0.51034 (11)	−0.1138 (7)	0.4144 (3)	0.0354 (11)
H12	0.490637	−0.199404	0.420407	0.042*
C13	0.50719 (10)	0.1103 (7)	0.4040 (3)	0.0288 (10)
C14	0.47504 (10)	0.2168 (9)	0.3989 (4)	0.0338 (11)
C15	0.44856 (10)	0.3023 (7)	0.3928 (3)	0.0336 (11)
C16	0.41605 (10)	0.3996 (7)	0.3822 (3)	0.0292 (10)
C17	0.38756 (10)	0.2721 (7)	0.3751 (3)	0.0344 (11)
H17	0.389718	0.117567	0.378542	0.041*
C18	0.35587 (11)	0.5760 (8)	0.3607 (4)	0.0413 (12)
H18	0.334343	0.639165	0.352911	0.050*
C19	0.41140 (11)	0.6223 (8)	0.3783 (4)	0.0435 (13)

H19	0.430383	0.714761	0.383682	0.052*
C30	0.05273 (11)	0.4922 (7)	0.6636 (3)	0.0424 (12)
H30	0.072646	0.576522	0.664071	0.051*
C31	0.02787 (11)	0.3870 (7)	0.6630 (3)	0.0326 (10)
C32	−0.00305 (9)	0.2642 (7)	0.6584 (3)	0.0285 (10)
C33	−0.00334 (12)	0.0375 (7)	0.6581 (4)	0.0365 (11)
H33	0.016966	−0.042556	0.660930	0.044*
C34	−0.03355 (11)	−0.0699 (8)	0.6536 (4)	0.0392 (11)
H34	−0.034419	−0.225118	0.653786	0.047*
C35	−0.06262 (11)	0.0523 (7)	0.6488 (3)	0.0363 (11)
H35	−0.083807	−0.017340	0.646112	0.044*
C36	−0.06015 (10)	0.2790 (7)	0.6481 (3)	0.0290 (10)
C37	−0.08946 (11)	0.4157 (8)	0.6394 (4)	0.0360 (12)
C38	−0.11320 (11)	0.5279 (8)	0.6289 (4)	0.0435 (12)
H38	−0.132307	0.618178	0.620414	0.052*
C20	0.29428 (9)	0.7296 (7)	0.5965 (4)	0.0318 (11)
H20	0.292990	0.884667	0.597844	0.038*
C21	0.32428 (10)	0.4171 (7)	0.5943 (4)	0.0330 (10)
H21	0.345516	0.347992	0.596533	0.040*
C22	0.26834 (10)	0.3858 (7)	0.5880 (4)	0.0349 (11)
H22	0.248720	0.298995	0.583860	0.042*
C23	0.26504 (9)	0.6106 (7)	0.5935 (3)	0.0269 (9)
C24	0.23295 (9)	0.7140 (7)	0.5960 (3)	0.0326 (10)
C25	0.20616 (10)	0.7997 (9)	0.5994 (4)	0.0346 (11)
C26	0.17343 (10)	0.8939 (7)	0.6015 (4)	0.0302 (10)
C27	0.14499 (9)	0.7674 (7)	0.6100 (4)	0.0367 (11)
H27	0.147299	0.613064	0.614459	0.044*
C28	0.11276 (11)	1.0713 (8)	0.6049 (4)	0.0417 (12)
H28	0.091100	1.134503	0.605115	0.050*
C29	0.16841 (11)	1.1186 (8)	0.5953 (4)	0.0419 (12)
H29	0.187305	1.211648	0.589241	0.050*

Atomic displacement parameters (Å²)

	U^{11}	U^{22}	U^{33}	U^{12}	U^{13}	U^{23}
N1	0.029 (2)	0.026 (2)	0.0311 (19)	−0.0023 (15)	0.0006 (16)	0.000 (2)
C1	0.029 (2)	0.042 (3)	0.064 (3)	−0.005 (2)	−0.001 (2)	−0.007 (3)
N2	0.030 (2)	0.036 (2)	0.042 (2)	−0.0029 (18)	0.0016 (17)	0.0004 (19)
C2	0.027 (2)	0.033 (3)	0.041 (3)	−0.009 (2)	0.000 (2)	−0.006 (2)
N3	0.033 (2)	0.027 (2)	0.052 (3)	0.0006 (18)	−0.0032 (18)	−0.005 (2)
C3	0.029 (2)	0.023 (2)	0.030 (2)	−0.0036 (18)	−0.0018 (19)	−0.003 (2)
N4	0.029 (2)	0.036 (2)	0.051 (3)	0.0002 (17)	0.0020 (18)	0.002 (2)
C4	0.045 (3)	0.026 (2)	0.035 (3)	−0.012 (2)	0.001 (2)	0.004 (2)
N5	0.036 (2)	0.032 (2)	0.073 (3)	0.0033 (19)	−0.007 (2)	0.003 (2)
C5	0.060 (3)	0.020 (2)	0.041 (3)	0.000 (2)	0.000 (2)	0.001 (3)
N10	0.029 (2)	0.022 (2)	0.033 (2)	−0.0026 (15)	0.0013 (15)	−0.0026 (19)
C6	0.044 (3)	0.024 (2)	0.043 (3)	0.006 (2)	−0.002 (2)	−0.001 (3)
N6	0.029 (2)	0.032 (2)	0.042 (2)	−0.0004 (16)	−0.0013 (18)	0.001 (2)

C7	0.034 (2)	0.024 (2)	0.027 (2)	0.0013 (19)	0.002 (2)	0.000 (2)
N7	0.0378 (19)	0.026 (2)	0.042 (2)	0.0024 (18)	−0.0013 (18)	−0.003 (2)
C8	0.030 (2)	0.031 (3)	0.036 (2)	0.004 (2)	0.000 (2)	0.001 (2)
N8	0.0276 (19)	0.037 (2)	0.046 (2)	0.0010 (17)	0.0017 (17)	−0.002 (2)
C9	0.031 (2)	0.040 (3)	0.049 (3)	0.001 (2)	0.000 (2)	−0.002 (3)
N9	0.033 (2)	0.032 (2)	0.074 (3)	0.0016 (18)	0.004 (2)	−0.004 (2)
C10	0.036 (2)	0.028 (3)	0.034 (3)	0.000 (2)	−0.0024 (18)	0.000 (2)
C11	0.030 (3)	0.036 (3)	0.047 (3)	0.008 (2)	0.003 (2)	−0.003 (2)
C12	0.033 (3)	0.031 (3)	0.042 (3)	−0.005 (2)	−0.004 (2)	−0.001 (2)
C13	0.025 (2)	0.033 (3)	0.028 (2)	0.0022 (19)	0.0020 (19)	−0.003 (2)
C14	0.032 (2)	0.037 (3)	0.033 (3)	0.001 (2)	0.000 (2)	−0.002 (2)
C15	0.032 (2)	0.038 (3)	0.030 (3)	0.002 (2)	−0.0017 (19)	−0.002 (2)
C16	0.028 (2)	0.031 (3)	0.029 (2)	0.0044 (18)	−0.0033 (17)	0.000 (2)
C17	0.035 (2)	0.030 (3)	0.039 (3)	0.002 (2)	0.0013 (19)	0.003 (2)
C18	0.033 (2)	0.043 (3)	0.048 (3)	0.011 (2)	0.000 (2)	0.003 (3)
C19	0.036 (3)	0.034 (3)	0.060 (3)	−0.004 (2)	−0.006 (2)	0.002 (3)
C30	0.031 (2)	0.048 (3)	0.048 (3)	−0.002 (2)	−0.002 (2)	−0.008 (2)
C31	0.031 (2)	0.032 (3)	0.034 (2)	0.008 (2)	0.0011 (19)	−0.001 (2)
C32	0.028 (2)	0.029 (2)	0.028 (2)	0.003 (2)	0.0002 (17)	0.001 (2)
C33	0.042 (3)	0.027 (2)	0.040 (3)	0.008 (2)	0.004 (2)	0.000 (3)
C34	0.057 (3)	0.018 (2)	0.042 (3)	0.001 (2)	0.001 (2)	0.003 (2)
C35	0.043 (3)	0.029 (3)	0.037 (3)	−0.007 (2)	0.000 (2)	0.001 (2)
C36	0.032 (2)	0.023 (2)	0.032 (3)	0.001 (2)	0.0018 (19)	−0.003 (2)
C37	0.028 (2)	0.036 (3)	0.044 (3)	−0.008 (2)	−0.001 (2)	−0.003 (2)
C38	0.029 (2)	0.041 (3)	0.060 (3)	0.002 (2)	−0.003 (2)	0.000 (3)
C20	0.033 (2)	0.025 (3)	0.036 (3)	0.002 (2)	0.001 (2)	0.001 (2)
C21	0.029 (2)	0.034 (3)	0.035 (2)	0.0079 (19)	0.003 (2)	0.000 (2)
C22	0.032 (2)	0.033 (3)	0.040 (3)	−0.004 (2)	−0.004 (2)	0.001 (2)
C23	0.025 (2)	0.030 (2)	0.026 (2)	0.0014 (18)	0.0002 (19)	0.003 (2)
C24	0.032 (2)	0.037 (3)	0.029 (2)	0.002 (2)	0.000 (2)	0.005 (2)
C25	0.034 (2)	0.037 (3)	0.032 (3)	0.003 (2)	0.000 (2)	0.004 (2)
C26	0.026 (2)	0.030 (2)	0.034 (2)	0.0014 (18)	−0.004 (2)	−0.002 (2)
C27	0.034 (2)	0.031 (3)	0.046 (3)	0.001 (2)	0.001 (2)	0.000 (3)
C28	0.028 (2)	0.041 (3)	0.056 (3)	0.006 (2)	0.003 (2)	−0.007 (3)
C29	0.032 (2)	0.033 (3)	0.061 (3)	−0.004 (2)	0.003 (2)	−0.005 (3)

Geometric parameters (Å, º)

N1—C3	1.339 (5)	C12—C13	1.383 (6)
N1—C7	1.348 (5)	C12—H12	0.9500
C1—C2	1.172 (6)	C13—C14	1.445 (6)
C1—H1	0.9500	C14—C15	1.185 (6)
N2—C11	1.333 (5)	C15—C16	1.438 (6)
N2—C10	1.339 (5)	C16—C19	1.376 (6)
C2—C3	1.445 (5)	C16—C17	1.385 (6)
N3—C11	1.324 (5)	C17—H17	0.9500
N3—C12	1.325 (5)	C18—H18	0.9500
C3—C4	1.394 (5)	C19—H19	0.9500

N4—C18	1.331 (5)	C30—C31	1.185 (6)
N4—C17	1.337 (5)	C30—H30	0.9500
C4—C5	1.389 (6)	C31—C32	1.450 (6)
C4—H4	0.9500	C32—C33	1.386 (6)
N5—C18	1.328 (5)	C33—C34	1.378 (6)
N5—C19	1.339 (5)	C33—H33	0.9500
C5—C6	1.370 (6)	C34—C35	1.385 (6)
C5—H5	0.9500	C34—H34	0.9500
N10—C36	1.338 (5)	C35—C36	1.389 (6)
N10—C32	1.340 (5)	C35—H35	0.9500
C6—C7	1.392 (6)	C36—C37	1.446 (6)
C6—H6	0.9500	C37—C38	1.180 (6)
N6—C20	1.334 (5)	C38—H38	0.9500
N6—C21	1.334 (5)	C20—C23	1.379 (5)
C7—C8	1.438 (5)	C20—H20	0.9500
N7—C21	1.328 (5)	C21—H21	0.9500
N7—C22	1.335 (5)	C22—C23	1.383 (6)
C8—C9	1.180 (6)	C22—H22	0.9500
N8—C28	1.334 (5)	C23—C24	1.433 (5)
N8—C27	1.338 (5)	C24—C25	1.195 (5)
C9—H9	0.9500	C25—C26	1.432 (5)
N9—C28	1.322 (5)	C26—C27	1.381 (5)
N9—C29	1.326 (5)	C26—C29	1.391 (6)
C10—C13	1.380 (5)	C27—H27	0.9500
C10—H10	0.9500	C28—H28	0.9500
C11—H11	0.9500	C29—H29	0.9500

C3—N1—C7	117.5 (4)	N5—C18—H18	116.3
C2—C1—H1	180.0	N4—C18—H18	116.3
C11—N2—C10	115.2 (4)	N5—C19—C16	122.9 (4)
C1—C2—C3	178.2 (5)	N5—C19—H19	118.5
C11—N3—C12	115.5 (4)	C16—C19—H19	118.5
N1—C3—C4	123.1 (4)	C31—C30—H30	180.0
N1—C3—C2	115.4 (4)	C30—C31—C32	177.4 (5)
C4—C3—C2	121.5 (4)	N10—C32—C33	122.9 (4)
C18—N4—C17	115.7 (4)	N10—C32—C31	115.5 (4)
C5—C4—C3	118.3 (4)	C33—C32—C31	121.7 (4)
C5—C4—H4	120.8	C34—C33—C32	118.9 (4)
C3—C4—H4	120.8	C34—C33—H33	120.5
C18—N5—C19	115.4 (4)	C32—C33—H33	120.5
C6—C5—C4	119.3 (4)	C33—C34—C35	118.9 (4)
C6—C5—H5	120.3	C33—C34—H34	120.5
C4—C5—H5	120.3	C35—C34—H34	120.5
C36—N10—C32	117.7 (4)	C34—C35—C36	118.6 (4)
C5—C6—C7	118.8 (4)	C34—C35—H35	120.7
C5—C6—H6	120.6	C36—C35—H35	120.7
C7—C6—H6	120.6	N10—C36—C35	123.0 (4)
C20—N6—C21	115.6 (4)	N10—C36—C37	115.7 (4)

N1—C7—C6	122.9 (4)	C35—C36—C37	121.3 (4)
N1—C7—C8	115.4 (4)	C38—C37—C36	177.8 (5)
C6—C7—C8	121.7 (4)	C37—C38—H38	180.0
C21—N7—C22	115.4 (4)	N6—C20—C23	122.5 (4)
C9—C8—C7	178.2 (5)	N6—C20—H20	118.7
C28—N8—C27	115.8 (4)	C23—C20—H20	118.7
C8—C9—H9	180.0	N7—C21—N6	127.3 (4)
C28—N9—C29	116.4 (4)	N7—C21—H21	116.3
N2—C10—C13	122.4 (4)	N6—C21—H21	116.3
N2—C10—H10	118.8	N7—C22—C23	122.7 (4)
C13—C10—H10	118.8	N7—C22—H22	118.6
N3—C11—N2	127.7 (4)	C23—C22—H22	118.6
N3—C11—H11	116.1	C20—C23—C22	116.4 (4)
N2—C11—H11	116.1	C20—C23—C24	121.9 (4)
N3—C12—C13	122.9 (4)	C22—C23—C24	121.7 (4)
N3—C12—H12	118.6	C25—C24—C23	179.1 (5)
C13—C12—H12	118.6	C24—C25—C26	177.5 (6)
C10—C13—C12	116.4 (4)	C27—C26—C29	116.0 (4)
C10—C13—C14	121.4 (4)	C27—C26—C25	122.1 (4)
C12—C13—C14	122.2 (4)	C29—C26—C25	121.9 (4)
C15—C14—C13	178.7 (5)	N8—C27—C26	122.5 (4)
C14—C15—C16	177.6 (5)	N8—C27—H27	118.7
C19—C16—C17	116.3 (4)	C26—C27—H27	118.7
C19—C16—C15	122.4 (4)	N9—C28—N8	126.8 (4)
C17—C16—C15	121.3 (4)	N9—C28—H28	116.6
N4—C17—C16	122.4 (4)	N8—C28—H28	116.6
N4—C17—H17	118.8	N9—C29—C26	122.5 (4)
C16—C17—H17	118.8	N9—C29—H29	118.8
N5—C18—N4	127.3 (4)	C26—C29—H29	118.8

Hydrogen-bond geometry (Å, º)

D—H···*A*	*D*—H	H···*A*	*D*···*A*	*D*—H···*A*
C10—H10···N3^{i}	0.95	2.50	3.423 (6)	165
C17—H17···N5^{ii}	0.95	2.49	3.420 (6)	166
C20—H20···N7^{i}	0.95	2.46	3.405 (6)	171
C27—H27···N9^{ii}	0.95	2.51	3.436 (6)	164
C1—H1···N4^{iii}	0.95	2.44	3.380 (6)	170
C5—H5···N1^{i}	0.95	2.38	3.331 (6)	176
C9—H9···N2	0.95	2.33	3.260 (5)	165
C30—H30···N8	0.95	2.47	3.380 (6)	160
C34—H34···N10^{ii}	0.95	2.39	3.336 (6)	175
C38—H38···N6^{iv}	0.95	2.32	3.268 (6)	175

Symmetry codes: (i) *x*, *y*+1, *z*; (ii) *x*, *y*−1, *z*; (iii) *x*+1/2, −*y*+1/2, *z*; (iv) *x*−1/2, −*y*+3/2, *z*.